Entropically driven self-assembly of multichannel rosette nanotubes

Hicham Fenniri*†, Bo-Liang Deng*, Alexander E. Ribbe*, Klaas Hallenga*, Jaby Jacob‡, and Pappannan Thiyagarajan‡

*1393 Herbert C. Brown Laboratory of Chemistry, Purdue University, West Lafayette, IN 47907-1393; and ‡Argonne National Laboratory, Intense Pulsed Neutron Source Division, 9700 South Cass Avenue, Argonne, IL 60439

Edited by Julius Rebek, Jr., The Scripps Research Institute, La Jolla, CA, and approved December 4, 2001 (received for review October 2, 2001)

Rosette nanotubes are a new class of organic nanotubes obtained through the hierarchical self-assembly of low molecular weight synthetic modules in water. Here we demonstrate that these materials can serve as scaffolds for the supramolecular synthesis of multichannel nanotubular architectures and report on the discovery of their entropy-driven self-assembly process.

Unidimensional nanotubular objects have captivated the minds of the scientific community over the past decade because of their boundless potential in nanoscale science and technology. The strategies developed to achieve the synthesis of these materials spanned the areas of inorganic (1–5) and organic (6–12) chemistry and resulted in, for instance, carbon nanotubes (1), peptide (9–11), and rosette nanotubes (12), as well as surfactant-derived tubular architectures (13–20). Although inorganic systems benefit from the vast majority of the elements of the periodic table and the rich physical and chemical properties associated with them, organic systems inherited the power of synthetic molecular (21, 22) and supramolecular (23, 24) chemistry. As such, the latter approach offers limitless possibilities in terms of structural, physical, and chemical engineering. Here, we present the design, self-assembly, and characterization of multichannel organic nanotubes in water and the discovery of their apparently entropy-driven self-assembly.

Design and Synthesis

The heteroaromatic bicyclic base **G**/**C** (Scheme 1), possessing the Watson–Crick donor-donor-acceptor of guanine and acceptor-acceptor-donor of cytosine, was recently reported in the context of the self-assembly of helical rosette nanotubes (12). Because of the disymmetry of its hydrogen bonding arrays, their spatial arrangement, and the hydrophobic character of the bicyclic system, **G**/**C** undergoes a hierarchical self-assembly process under physiological conditions to form a six-membered supermacrocycle maintained by 18 H-bonds (Fig. 1 *Upper*, thin solid bars). The resulting and substantially more hydrophobic aggregate then undergoes a second level of organization to produce a stack. The architecture thus generated defines an unoccluded central pore running the length of the stack with tunable inner and outer diameters (Fig. 1 *Lower*). The inner space is directly related to the distance separating the H-bonding arrays within **G**/**C**, whereas the peripheral diameter and its chemistry are dictated by the choice of the functional groups conjugated to this motif.

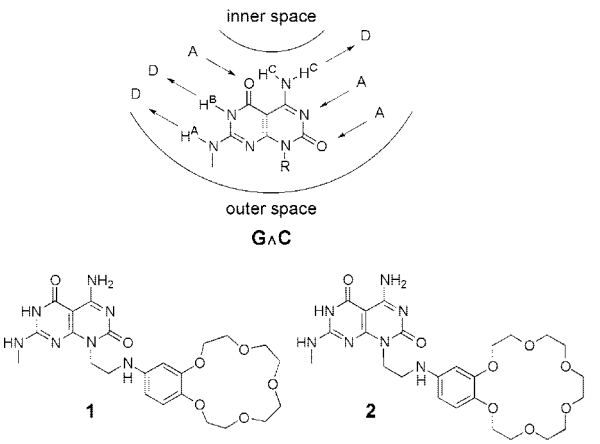

Scheme 1. **G**/**C** motif and compounds **1** and **2** synthesized. Detailed experimental procedures for the preparation of all of the intermediates and final compounds along with the corresponding spectroscopic characterizations are in the supporting *Methods* and Fig. 6.

In addition to their demonstrated synthetic accessibility and broad solvent compatibility, crown ethers are a very versatile class of receptors that display size, shape, and charge selectivity toward their guests (25). Furthermore, extensive investigations were carried out to establish their ionophoric properties (25) and incorporate them in artificial channel systems (26, 27), molecular photonic (28–30), and electronic (31, 32) devices. In the present article, **1** and **2** were synthesized and investigated to establish the rosette nanotubes as stable, yet noncovalent scaffolds for the self-organization of multichannel assemblies (Fig. 1). We also demonstrate that the presence of cations known to coordinate to crown ethers does not affect the one-dimensional organization, thereby reinforcing the potential of these materials in the design of iono-, photo-, and electro-active nanotubes and nanowires as well as in the preparation of selective ion channels. While investigating the mechanism of their formation, we also have uncovered their peculiar response to temperature, which strongly supports the entropic nature of the assembly process.

A synthetic scheme was devised to allow for the preparation of **1** and **2** and the functionalization at virtually any position (Scheme 1). The versatility of the synthetic strategy allows for the incorporation of a wide range of crown ether hosts differing in dimensions and properties. All of the compounds were characterized by ^{1}H NMR, ^{13}C NMR, and MS. In addition, the key intermediates were characterized by high-resolution MS and

This paper results from the Arthur M. Sackler Colloquium of the National Academy of Sciences, ''Nanoscience: Underlying Physical Concepts and Phenomena,'' held May 18–20, 2001, at the National Academy of Sciences in Washington, DC.

This paper was submitted directly (Track II) to the PNAS office.

Abbreviations: NOE, nuclear Overhauser effect; DLS, dynamic light scattering; SAXS, small angle x-ray scattering; TEM, transmission electron microscopy; 2D, two-dimensional; FT, Fourier transform; fb, flip-back.

†To whom reprint requests should be addressed. E-mail: hf@purdue.edu.

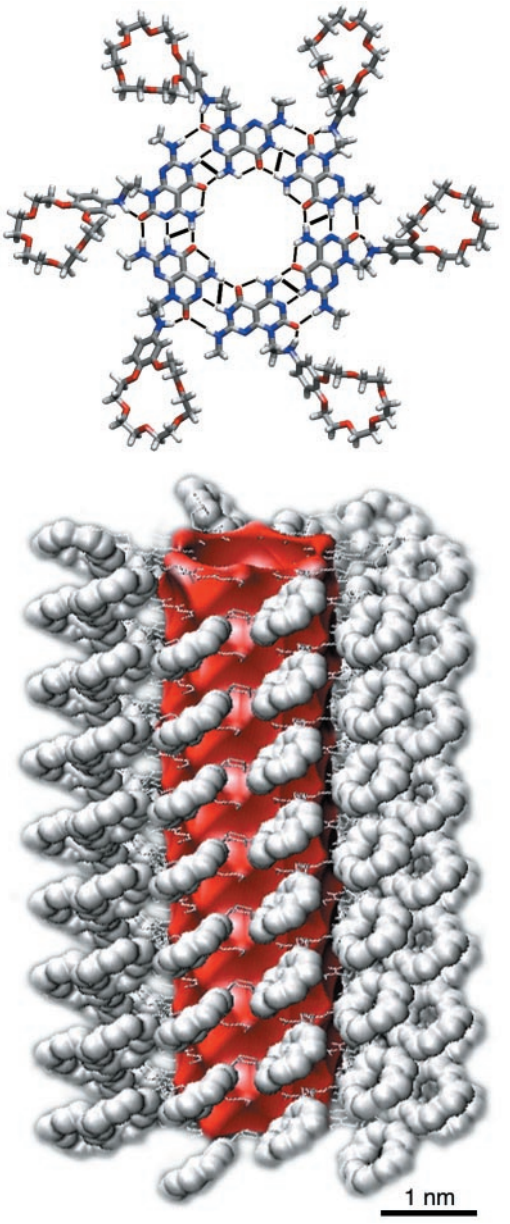

Fig. 1. Hierarchical self-assembly of compound **2** into a multichannel rosette nanotube (MACROMODEL, version 7.2) (see supporting *Methods*).

elemental analysis (see additional *Methods* and Fig. 6, which are published as supporting information on the PNAS web site, www.pnas.org).

NMR Studies

One-dimensional experiments (600 MHz, 90% H_2O/D_2O) between 2°C and 42°C indicated broadening at all but the lowest temperatures. A major and a minor population of imino protons coexist with a ratio of 3:1, which is independent of concentration (0.001 to 0.025 M) and temperature (2–42°C) (see supporting *Methods* and Fig. 7, which is published as supporting information on the PNAS web site). Flip-back total correlation spectroscopy (fb-TOCSY), nuclear Overhauser effect (NOE) spectroscopy (NOESY), and rotating frame Overhauser effect spectroscopy (ROESY) experiments were then carried out on the same solution to establish the self-assembly of the rosette supermacrocycle and to gain further information about the nature of the two coexisting species. fb-TOCSY experiments did not show any cross-peak between the imino protons, except an exchange NOE between the minor and major ^{A}H resonances. fb-NOESY experiments showed the expected cross-peaks between, respectively, the major and minor ^{B}H and ^{C}H resonances, which were confirmed by fb-ROESY as nonchemical exchange NOEs. Because ^{B}H and ^{C}H are too far apart to display any intramodular NOEs, the observation of an NOE between them corroborates the formation of intermodular H-bonds as highlighted in Fig. 1 (*Upper*, thick solid bars). The fb-NOESY also revealed the expected cross-peak between the minor ^{A}H and ^{B}H but not between the major ^{A}H and ^{B}H resonances, thereby suggesting that the major $CH_3{}^{A}H$ protons are in a nonhydrogen-bonded conformation. Such conformation apparently would place $CH_3{}^{A}H$ away from ^{B}H (see supporting *Methods* and Figs. 8 and 9, which are published as supporting information on the PNAS web site).

Variable Temperature UV-Visible Studies

The electronic spectra of **1** and **2** display a profile typical of the DNA bases, with two maxima at 238 nm and 287 nm. A strong indicator of DNA stability and tertiary structure is the hyperchromicity observed upon its denaturation (33). In this regard the supramolecular outcome of **1** and **2** was anticipated to behave similarly as was shown in the case of a lysine-substituted module (12). This hypothesis did not hold in the case of **1** and **2**. The spectra displayed a linear, noncooperative, irreversible, and small hyperchromic effect in the range of 25°C to 95°C, regardless of the presence of sodium or potassium (up to 10 equivalents). Furthermore, the UV-visible spectra of 4-aminobenzo-18-crown-6-ether (18C6) remain essentially unaffected in this temperature range with or without potassium (see supporting *Methods*, Fig. 10, and Table 2, which are published as supporting information on the PNAS web site). To rationalize this data we postulated that the supramolecular outcome of **1** and **2** must be unusually stable in the temperature range of 25°C to 95°C, despite its noncovalent nature. Variable temperature dynamic light scattering (DLS), small angle x-ray scattering (SAXS), and transmission electron microscopy (TEM) proved to be the ideal tools to probe this hypothesis.

DLS and SAXS Studies

To assess the hydrodynamic dimensions (length and diameter) of the proposed nanotubes**,** DLS and SAXS measurements were carried out on dilute aqueous solution of **1** and **2** (see supporting *Methods* and Fig. 11, which is published as supporting information on the PNAS web site). A narrow monomodal distribution (>90% in the range of 12 to 42 nm) with an average apparent hydrodynamic radius, R_H, of 16.0 nm for **1** and 26.7 nm for **2** was recorded by DLS at 20°C. The 15C5 crown ether of compound **1** is known to bind Na^+ selectively. DLS and SAXS studies (Table 1) performed on **1** in the absence and presence of Na^+ (up to 10 equivalents) indicate that the latter does not alter the dimensions of the resulting assembly in solution (R_H = 16 nm, diameter ≈4 nm). The same conclusions can be drawn for compound **2** on the basis of the DLS, SAXS, and TEM data. Finally, owing to the hydrophobic character of the nanotubes' core, the consistently lower diameter derived from the SAXS data may reflect the more compact state of the assembly in water. Note also that the TEM measurements include a layer of the staining agent, whereas the computed diameter takes into consideration the energy-minimized (fully expanded) conformation of the crown ethers.

The most impressive and unexpected observation was the peculiar and unprecedented response of these materials to temperature. As the latter increased so did the length of the nanotubes. In the range of 20°C to 40°C, the average hydrody-

Table 1. Dimensions of the nanotubes generated from 1 and 2 determined by DLS, SAXS, and TEM

	DLS,* R_H, nm	SAXS,† diameter, nm	TEM,‡ diameter, nm	Computed§ diameter, nm
1	16.0	3.6 ± 0.66	3.9 (3.9)	4.0
1 + NaCl	17.0	4.13 ± 0.70	4.2 (4.1)	4.0
1 + KCl	17.0	3.71 ± 0.47	4.0 (3.9)	4.0
2	26.7	—	4.5 (4.4)	4.3
2 + NaCl	27.0	3.5 ± 0.09¶	4.4 (4.5)	4.3
2 + KCl	27.0	3.5 ± 0.09¶	4.4 (4.4)	4.3

*[**1**] = [**2**] = [NaCl] = [KCl] = 2×10^{-3} M in water.

†[**1**] = [**2**] = [NaCl] = [KCl] = 1.3×10^{-3} M in water at 20°C.

‡[**1**] = [**2**] = [NaCl] = [KCl] = 2×10^{-4} M in water. The numbers in parentheses were recorded for the same aqueous samples after incubation at 70°C for 30 min in a thermostated bath. All the outer diameters include a layer of the staining agent and are each an average of 100 measurements made on randomly selected nanotubes. These numbers were also confirmed by using 2D-FT of densely packed nanotubes (see Fig. 5).

§Computer models generated by using MACROMODEL 7.2.

¶Measurement performed in 10 mM Mes buffer, pH 5.5. This solution contains a 5-fold excess of sodium and potassium with respect to **2**. In the absence of the Mes buffer the data was not reproducible.

namic radius grew over 320% for both **1** and **2** (Fig. 2). Above 40°C the increased scattering from larger assemblies saturated the detector of the instrument used.

As most self-assembly processes involving noncovalent interactions are enthalpically driven and entropically unfavorable, the increased and controlled level of aggregation as the temperature increases was the most significant observation in this study. This behavior is reminiscent of the hydrophobic effect, in which release of ordered water to the bulk solvent contributes to the solute's self-association. Entropically driven self-assembly processes in aqueous solutions are well known in natural systems (34–38), for colloidal microparticles (39), and in few instances for small molecules in organic solvents (40, 41). There is, however, no precedent of such process for well-defined nanoscale synthetic assemblies in water. In the present case, we believe that ordered water molecules on the hydrophobic surfaces of the bases located on each end of the nanotubes are released to the bulk solvent as the temperature increases while new rosette stacks are being recruited. This process would result in elongated nanotubes, in agreement with the DLS data (Fig. 2).

TEM Studies

TEM provided us with visual evidence of the formation of the proposed nanotubular assemblies, a confirmation of their dimensions, and the temperature effect recorded by DLS. Fig. 3 shows negatively stained samples of the nanotubes derived from **1** and **2**. Detailed analysis of these micrographs led to the following conclusions: (*i*) all of the assemblies have the same outer diameter (≈ 4 nm), in agreement with the computed one (Table 1). (*ii*) Sodium or potassium did not alter the dimensions nor the tubular organization, also in agreement with the DLS and SAXS data. (*iii*) Temperature annealing does not affect the nanotubes' diameter. (*iv*) In agreement with the variable temperature DLS studies, the density of the nanotubular assemblies increased dramatically with temperature, thereby highlighting the entropic nature of the self-assembly process. In effect, as macromolecular systems enter the high nanometer to low micrometer regime, attractive long-range, inter-particle forces (also called depletion forces or colloid interactions) (39) become relatively significant, thereby leading once again to release of ordered solvent molecules to the bulk and resulting in a new level of aggregation under the effect of temperature (phase separation). This property is fundamental to colloid science, namely,

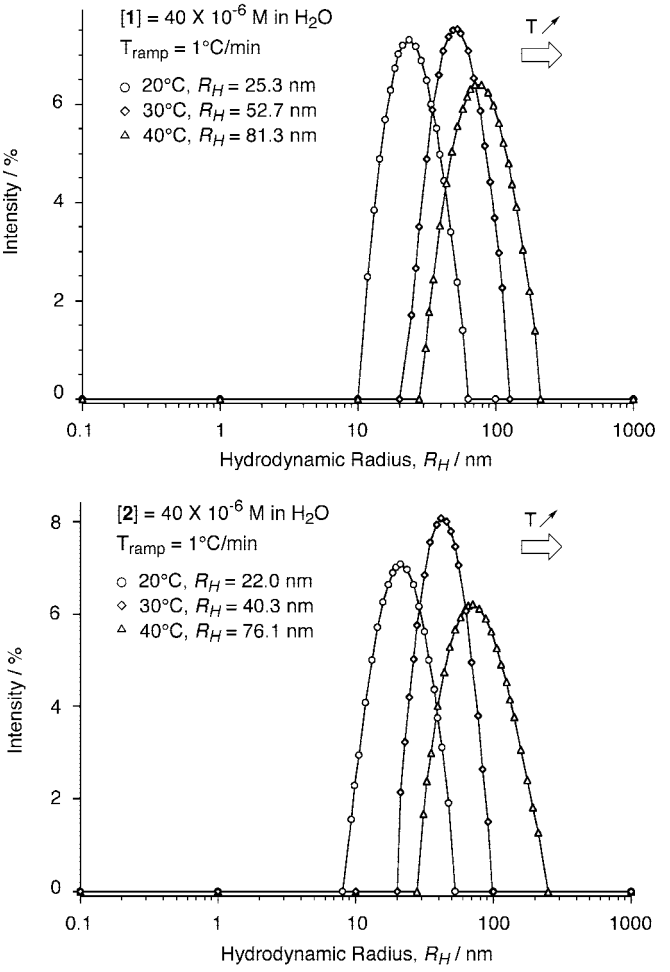

Fig. 2. DLS regularization diagrams of 40×10^{-6} M solutions of **1** (*Upper*) and **2** (*Lower*) in H_2O at 20°C, 30°C, and 40°C. The average hydrodynamic radii recorded are shown (see supporting *Methods*).

there is always an attractive force between like particles in solution, tending to induce aggregation (42). This is also the essence of van der Waals forces applied to aggregates of molecules, rather than between individual molecules.

Concentrated samples of **1** or **2** generally result in higher density areas of nanotubes on the carbon-coated TEM grids that allowed us to extract information about their hollow nature, as well as their propensity to undergo a grid-like organization over multiple layers. Shown in Fig. 4 is an area of the TEM image where hollow, disk-shaped entities are identified. A remarkable feature of this image is that these objects appear to have been borne out of a parent nanotube as most of them seem to follow a linear organization. Furthermore, judging from their dimensions, we are indeed compelled to conclude that these entities are the rosette components that make up the nanotubular assemblies. Finally, two-dimensional (2D)-Fourier transform (FT) studies of the TEM images of densely packed rosette nanotubes (Fig. 5) allowed us to reveal their propensity to pack into multiple-layer thin films with quasi-perpendicular grid-like organization, thereby offering a new level of control over the supramolecular outcome of compounds **1** and **2**.

Conclusion

The self-assembly of type I collagen fibrils (34, 35), the polymerization of the coat protein of the tobacco mosaic virus (36), and the self-assembly of bovine brain tubulin (37) or β-amyloids

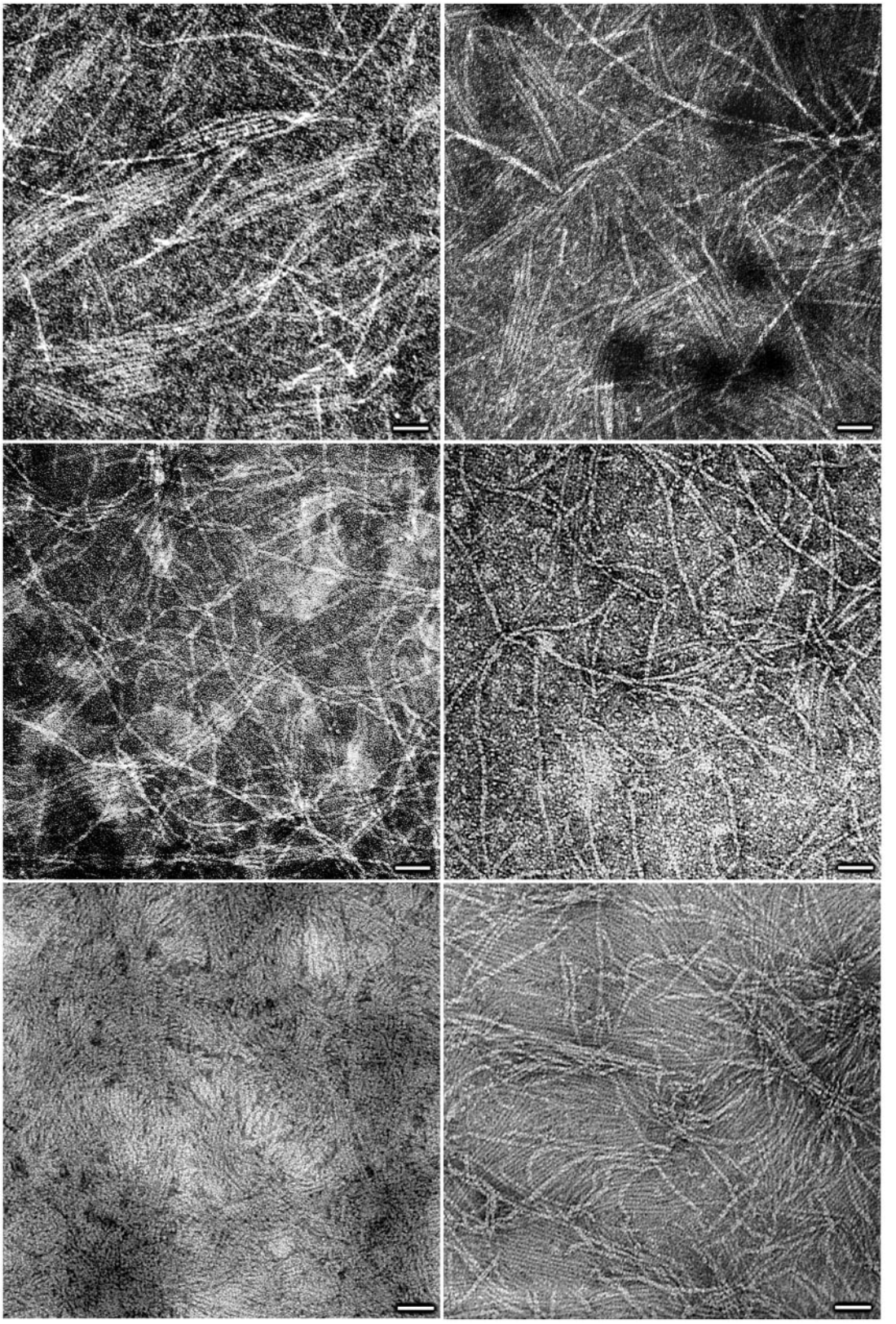

Fig. 3. Transmission electron micrographs of negatively stained samples of **1** and **2** (*Top*, left to right), **1** + NaCl and **2** + KCl (*Middle*, left to right), and **2** annealed in the absence and presence of KCl (*Bottom*, left to right). (Scale bar = 40 nm.) See supporting *Methods*.

(38) are just a few classical examples of entropy-driven processes from nature. The discovery of the same behavior in the process of rosette nanotubes' self-assembly offers opportunities not only for in-depth structural and thermodynamic studies of this phenomenon, but also an additional tool in supramolecular engineering. Indeed, this study has many implications on our ability

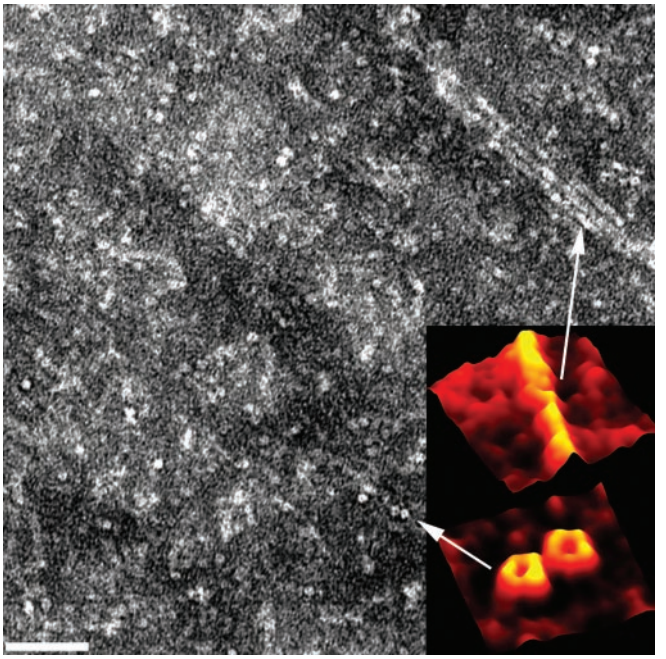

Fig. 4. Transmission electron micrograph featuring top views of the nanotubes and revealing their hollow nature. (*Inset*) Three-dimensional reconstructions of the gray value profiles derived from the TEM images by using the National Institutes of Health program IMAGE. (Scale bar = 40 nm.) See supporting *Methods*.

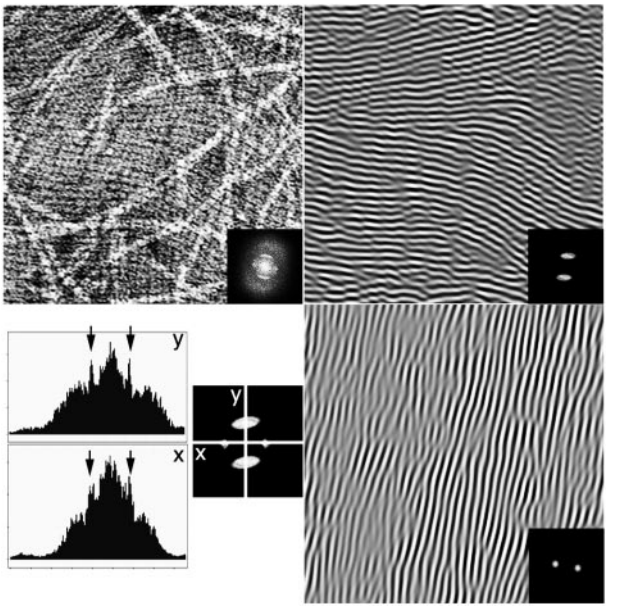

Fig. 5. 2D-FT analysis of a densely packed multiple layer thin film of nanotubes generated from **1**. Transmission electron micrograph of multiple layers of nanotubes obtained from **1** (magnification: ×35,000) and original 2D-FT (*Inset*) (*Upper Left*). Inverse 2D-FT of masked 2D-FT (*Inset*) revealing the first densely packed nanotube layer oriented horizontally (*Upper Right*). Inverse 2D-FT of masked 2D-FT (*Inset*) revealing a second nanotube layer oriented vertically (*Lower Right*). 2D-FT profile along the *x* and *y* axes showing the quasi-perpandicularity of the two layers (*Lower Left*).

to control the elusive hydrophobic effect, as it is a demonstration that H-bonds can be recruited to orchestrate an entropically fueled process.

This article establishes that nanotubular constructs resulting from the self-assembly of the **G**/**C** motif can serve as noncovalent, yet very stable, scaffolds for the supramolecular synthesis of multichannel assemblies and unfolds the generality of the hierarchical self-assembly approach to functional nanotubular assemblies with predefined properties. In effect, further elaboration of the outer surface of this motif can result in unidimensional assemblies with predefined chemical and physical properties.

We acknowledge the support of the National Science Foundation (Career Award), the American Cancer Society (Grant ACS-IRG 58), the American Chemical Society-Petroleum Research Fund, the Showalter Foundation, the 3M Company, and Purdue University. H.F. is a Cottrell Scholar of Research Corporation.

1. Iijima, S. (1991) *Nature (London)* **354,** 56–58.
2. Hamilton, E. J. M., Dolan, S. E., Mann, C. M., Colijin, H. O., McDonald, C. A. & Shore, S. G. (1993) *Science* **260,** 659–661.
3. Brumlik, C. J. & Martin, C. R. (1991) *J. Am. Chem. Soc.* **113,** 3174–3175.
4. Shenton, W., Douglas, T., Young, M., Stubbs, G. & Mann, S. (1999) *Adv. Mater.* **11,** 253–256.
5. Chopra, N. G., Luyken, R. J., Cherrey, K., Crespi, V. H., Cohen, M. L., Louie, S. G. & Zettl, A. (1995) *Science* **269,** 966–967.
6. Harada, A., Li, J. & Kamachi, M. (1993) *Nature (London)* **364,** 516–518.
7. Nelson, J. C., Saven, J. G., Moore, J. S. & Wolynes, P. G. (1997) *Science* **277,** 1793–1796.
8. Ashton, P. R., Brown, C. L., Menzer, S., Nepogodiev, S. A., Stoddart, J. F. & Williams, D. J. (1996) *Chem. Eur. J.* **2,** 580–591.
9. Bong, D. T., Clark, T. D., Granja, J. R. & Ghadiri, M. R. (2001) *Angew. Chem. Int. Ed.* **40,** 988–1011.
10. Ranganathan, D., Lakshmi, C. & Karle, I. L. (1999) *J. Am. Chem. Soc.* **121,** 6103–6107.
11. Seebach, D., Matthews, J. L., Meden, A., Wessels, T., Baerlocher, C. & McCusker, L. B. (1997) *Helv. Chim. Acta* **80,** 173–181.
12. Fenniri, H., Mathivanan, P., Vidale, K. L., Sherman, D. M., Hallenga, K., Wood, K. V. & Stowell, J. G. (2001) *J. Am. Chem. Soc.* **123,** 3854–3855.
13. Schnur, J. M. (1993) *Science* **262,** 1669–1676.
14. Nakashima, N., Asakuma, S. & Kunitake, T. (1985) *J. Am. Chem. Soc.* **107,** 509–510.
15. Fuhrhop, J.-H., Spiroski, D. & Boettcher, C. (1993) *J. Am. Chem. Soc.* **115,** 1600–1601.
16. Frankel, D. A. & O'Brien, D. F. (1994) *J. Am. Chem. Soc.* **116,** 10057–10069.
17. Imae, T., Takahashi, Y. & Maramatsu, H. (1992) *J. Am. Chem. Soc.* **114,** 3414–3419.
18. Kimizuka, N., Fujikawa, S., Kuwahara, S., Kunitake, T., Marsh, A. & Lehn, J.-M. (1995) *Chem. Commun.* 2103–2104.
19. Klok, H.-A., Joliffe, K. A., Schauer, C. L., Prins, L. J., Spatz, J. P., Möller, M., Timmerman, P. & Reinhoudt, D. N. (1999) *J. Am. Chem. Soc.* **121,** 7154–7155.
20. Choi, I. S., Li, X., Simanek, E. E., Akaba, R. & Whitesides, G. M. (1999) *Chem. Mat.* **11,** 684–690.
21. Corey, E. J. & Cheng, X.-M. (1989) *The Logic of Chemical Synthesis* (Wiley, New York).
22. Nicolaou, K. C. & Sorensen, E. J. (1996) *Classics in Total Synthesis* (VCH, New York).
23. Whitesides, G. M., Simanek, E. E., Mathias, J. P., Seto, C. T., Chin, D. N., Mammen, M. & Gordon, D. M. (1995) *Acc. Chem. Res.* **28,** 37–44.
24. Prins, L. J., Reinhoudt, D. N. & Timmerman, P. (2001) *Angew. Chem. Int. Ed.* **40,** 2382–2426.
25. Dietrich, B., Viout, P. & Lehn, J.-M. (1993) *Macrocyclic Chemistry: Aspects of Organic and Inorganic Supramolecular Chemistry* (VCH, Weinheim, Germany).
26. Biron, E., Voyer, N., Meillon, J. C., Cormier, M.-E. & Auger, M. (2000) *Biopolymers Pep. Sci.* **55,** 3364–3372.
27. Roks, M. F. M. & Nolte, R. J. M. (1992) *Macromolecules* **25,** 5398–5407.
28. Engelkamp, H., Middelbeek, S. & Nolte, R. J. M. (1999) *Science* **284,** 785–788.
29. Meillon, J.-C., Voyer, N., Biron, E., Sanschagrin, F. & Stoddart, F. (2000) *Angew. Chem. Int. Ed.* **39,** 143–145.
30. Balzani, V., Credi, A. & Venturi, M. (1998) *Coord. Chem. Rev.* **171,** 3–16.
31. Balzani, V., Credo, A., Raymo, F. M. & Stoddart, J. F. (2000) *Angew. Chem. Int. Ed.* **39,** 3348–3391.
32. Ballardini, R., Balzani, V., Credi, A., Gandolfi, M. T. & Venturi, M. (2001) *Acc. Chem. Res.* **34,** 445–455.

33. Cantor, C. R. & Schimmel, P. R. (1980) *Biophysical Chemistry* (Freeman, New York).
34. Kadler, K. E., Hojima, Y. & Prockop, D. J. (1987) *J. Biol. Chem.* **262,** 15696–15701.
35. Kadler, K. E., Hojima, Y. & Prockop, D. J. (1988) *J. Biol. Chem.* **263,** 10517–10523.
36. Riedhoff, P., Schneider, A., Mandelkow, E.-M. & Mandelkow, E. (1998) *Biochemistry* **37,** 10223–10230.
37. Karr, T. L. & Purich, D. L. (1980) *Biochem. Biophys. Res. Commun.* **95,** 1885–1889.
38. Shalaby, R. A. & Lauffer, M. A. (1985) *Arch. Biochem. Biophys.* **236,** 390–398.
39. Yodh, A. G., Lin, K.-H., Crocker, J. C., Dinsmore, A. D., Verma, R. & Kaplan, P. D. (2001) *Philos. Trans. R. Soc. London A* **359,** 921–937.
40. Kang, J. & Rebek, J., Jr. (1996) *Nature (London)* **382,** 239–241.
41. Schmuck, C. (2001) *Tetrahedron* **57,** 3063–3067.
42. Hemsley, A. R. & Griffiths, P. C. (2000) *Philos. Trans. R. Soc. London A* **358,** 547–564.